
QUANTITATIVE ASSESSMENT OF MATERIAL HETEROGENEITY
USING ACOUSTIC MICROSCOPY

BY

GALE ANN BRIGHT

B.S., University of Illinois, 1980

THESIS

Submitted in partial fulfillment of the requirements
for the degree of Master of Science in Electrical Engineering
in the Graduate College of the
University of Illinois at Urbana-Champaign, 1982

Urbana, Illinois

TABLE OF CONTENTS

CHAPTER		Page
1	INTRODUCTION.	1
2	MEASUREMENT TECHNIQUES.	4
	2.1 SPEED OF SOUND	4
	2.2 ROLE OF THE DATA ACQUISITION SYSTEM.	7
	2.3 THE FILTER	12
	2.4 CALCULATION OF THE SPEED OF SOUND USING AUTOMATED PROGRAM.	13
3	METHODS OF PREPARATION.	23
	3.1 SPECIMEN PREPARATION	23
	3.2 MICROSCOPE PREPARATION	26
	3.3 DATA COLLECTION.	29
4	ERROR ANALYSIS.	34
5	RESULTS AND DISCUSSION.	42
	APPENDIX - DATA COLLECTING PROGRAM	50
	REFERENCES	56

CHAPTER 1

INTRODUCTION

The Scanning Laser Acoustic Microscope, SLAM, is a sophisticated ultrasonic device located at the Bioacoustics Research Laboratory, in the Department of Electrical Engineering, University of Illinois at Urbana-Champaign. It is an instrument that is used to investigate the elastic and viscoelastic properties of materials at the microscopic level by means of quantitative measures of the acoustic speed and ultrasonic attenuation coefficient. Microscopic measures of these ultrasonic propagation properties are not available when using conventional optical microscopy as light waves do not interact directly with the mechanical properties of a specimen but rather with its dielectric properties.

As implied by its name, the SLAM employs a scanning laser and sound waves. Sound waves are generated at 100 MHz beneath the stage of the microscope and directed through the stage towards the specimen which is placed on its top. The sound passes through the specimen and is incident upon the lower surface of a specially designed coverslip placed on top of the specimen. The laser scans, in a raster fashion, the surface of the coverslip (an approximately 3 mm x 2 mm area) detecting mechanical disturbances induced into the coverslip. Through processing of the reflected scanned laser beam an acoustic micrograph is constructed and displayed on a television monitor.

The SLAM has been used to investigate a variety of materials from wound tissue (O'Brien, et al., 1981) to detection of flaws in integrated circuits (Kessler, 1979). SLAM allows tissue to be examined without using fixatives or stains to enhance certain structures as is often necessary in optical microscopy. This staining can change the very structures that need to be investigated in their natural state. However, it may be possible for mechanical staining to enhance structures which otherwise may be difficult to investigate using the SLAM.

The resolution of the SLAM at 100 MHz ranges from 15-60 micrometers depending upon the wavelength of sound in the material being examined. An important consideration at such a high frequency is that the total insertion loss of sound in materials can increase significantly with increasing thickness. Thus, the thickness of the specimen must be such that the detected acoustic signal falls within the SLAM's dynamic range.

The SLAM has been interfaced to the laboratory's Perkin-Elmer 7/32 mini-computer (Foster, 1981) and thus enabled the digitization of the acoustic image from the video signal from which appropriate signal processing is possible. Attenuation measurements have been semi-automated (i.e., require little operator input - Mravca, 1981), but the same has not true been for the speed of sound determinations. Prior to this project, a substantial portion of the acoustic velocity determination was performed manually and with less

precision than that which would be expected if one were using a computer assisted technique. Thus the aim of this project was to automate the speed of sound calculations and also investigate some statistical parameters which had yet to be considered.

CHAPTER 2

MEASUREMENT TECHNIQUES

2.1 SPEED OF SOUND

The Scanning Laser Acoustic Microscope is capable of providing the necessary information to determine the speed of sound in an object. Specifically, the SLAM must be operating in the interference mode. Imagine two plane waves (one passing through the specimen and the other through a homogeneous media) with the same frequency, traveling at an angle θ with respect to each other, impinging upon the coverslip of the microscope. Upon intersection, the two beams constructively and destructively interfere with each other. In practice, this mode is made available by electronic mixing of the acoustic image detector signal with an internal reference signal. The end result is approximately 39 evenly spaced vertical fringe lines displayed on the television monitor (Figure 2.1 a). Placing an object in the path of one of the two beams results in a localized lateral shift of the fringe lines (Figure 2.2). This shift is actually the difference of the acoustic speeds of the two sound waves, one of which is now traveling in a new medium.

The calculation of the speed of sound in a specimen is found using a formula derived in a paper by Goss and O'Brien (1979):

$$C_x = \frac{C_o}{\sin\theta_o} \sin \left[\tan^{-1} \left(\frac{1}{1/\tan\theta_o - (N\lambda_o/T\sin\theta_o)} \right) \right] \quad (1)$$

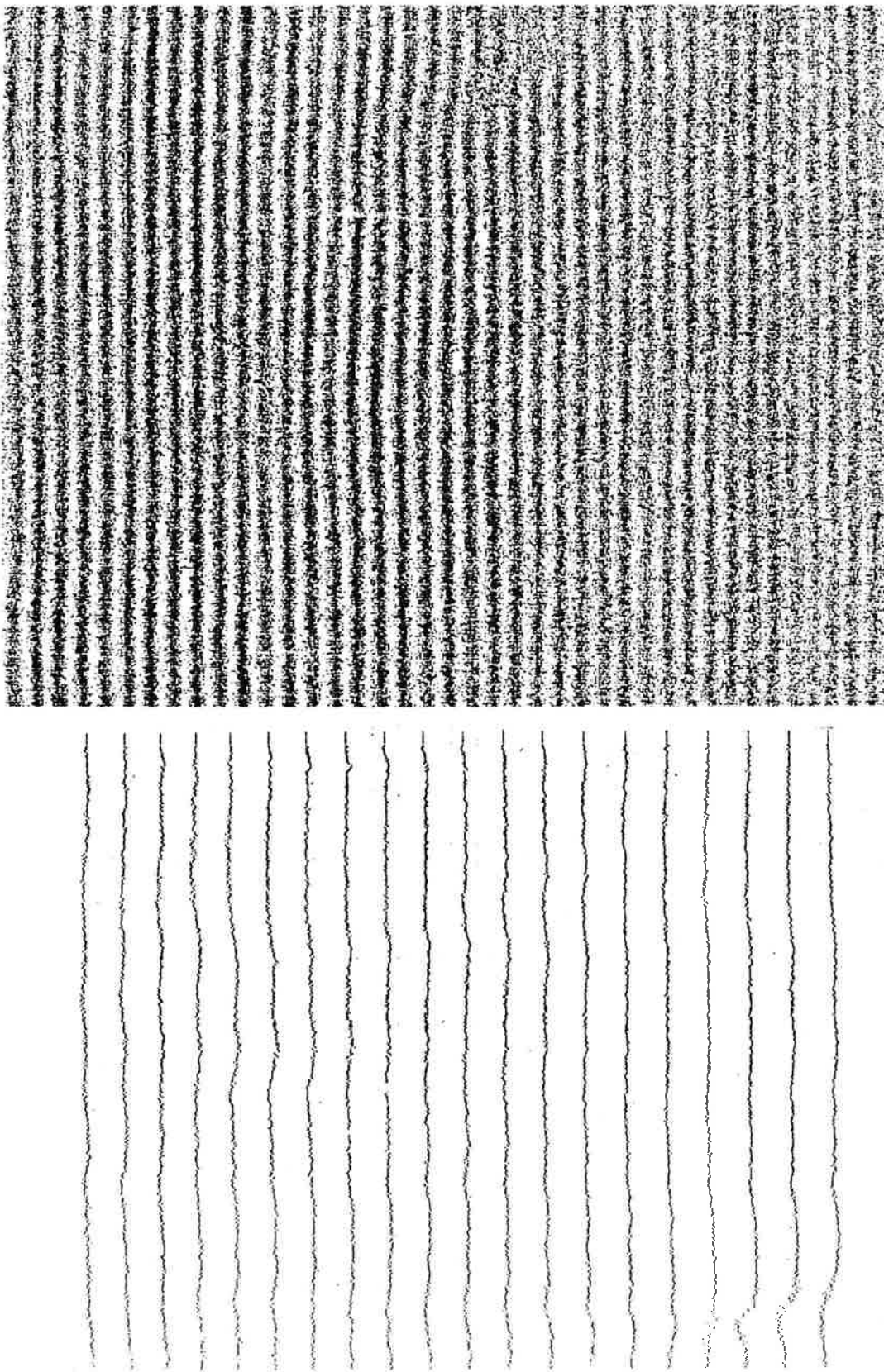


Figure 2.1 a) (upper) interference image as digitized
resembling television monitor
b) (lower) correlated interference image
of the right hand portion of (a).

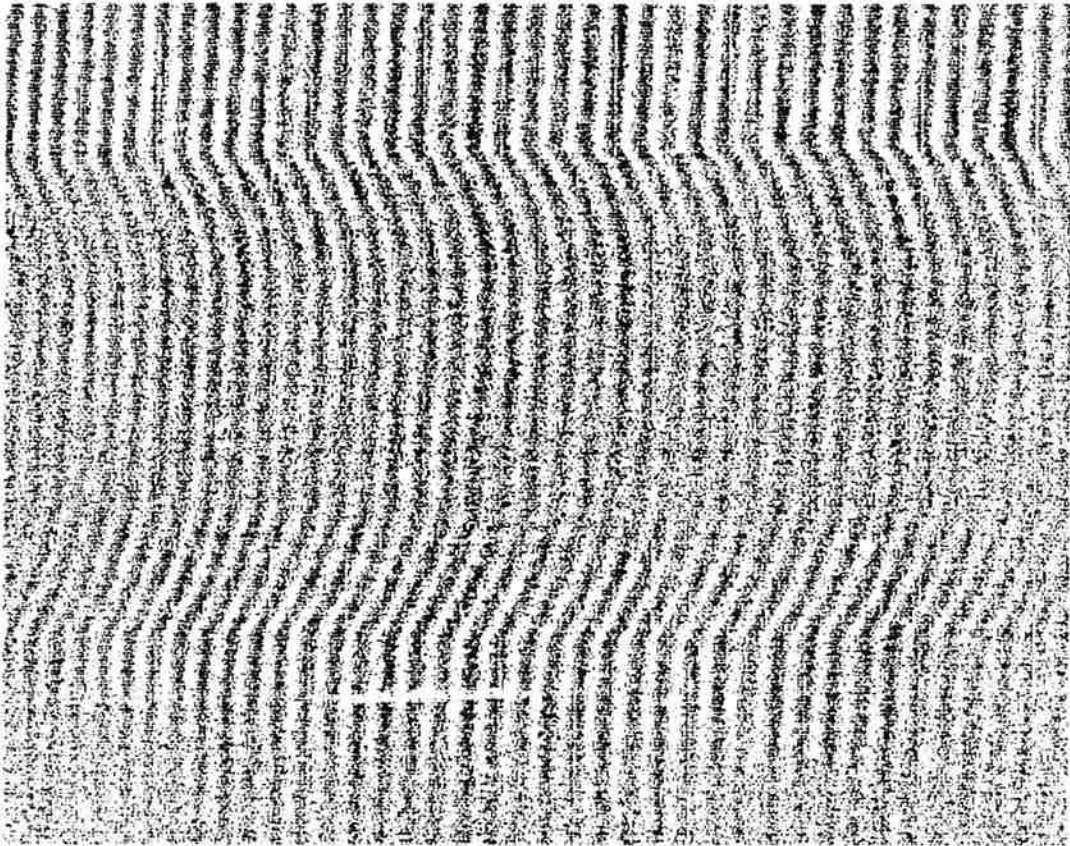


Figure 2.2 Interference image illustrating the fringe shift which occurs when an object is in the field of view of the SLAM.

where C_o is the speed of sound in the surrounding reference medium, λ_o is the wavelength of sound in that same medium, θ_o is the angle of the beam from the normal in the surrounding medium, T is the thickness of the object, and N is the normalized lateral fringe shift (ab/ac - see Figure 2.3). Using Snell's Law, θ_o can be determined for the reference medium.

$$\theta_o = \sin^{-1} \left[\frac{C_o}{C_s} \sin \theta_s \right] \quad (2)$$

where C_s is the speed of sound in the silica stage (5968 m/s) and θ_s is the angle at which the generated sound waves travel through the stage with respect to the normal ($\theta_s = 45^\circ$). In this project, the materials being examined are biological specimens; therefore saline solution (0.9 % concentration) is used as the reference medium. This saline solution is isotonic with the specimens and allows the specimens to retain their normal osmolarity. Saline has a known speed of 1507 m/s (Goss and O'Brien, 1979), hence $\theta_o = 10.2^\circ$.

2.2 ROLE OF THE DATA ACQUISITION SYSTEM

The interference image produced by the SLAM is digitized using a Data Acquisition System, DAS, designed at the Bioacoustics Research Lab (Foster, 1981) capable of digitizing the video signal from the SLAM for use with the Perkin-Elmer 7/32, a 32-bit mini-computer. The DAS (Figure 2.4) consists of an rf amplifier, a 28.6 MHz (8 bit) analog to digital (A/D) converter, and a high speed buffer memory.

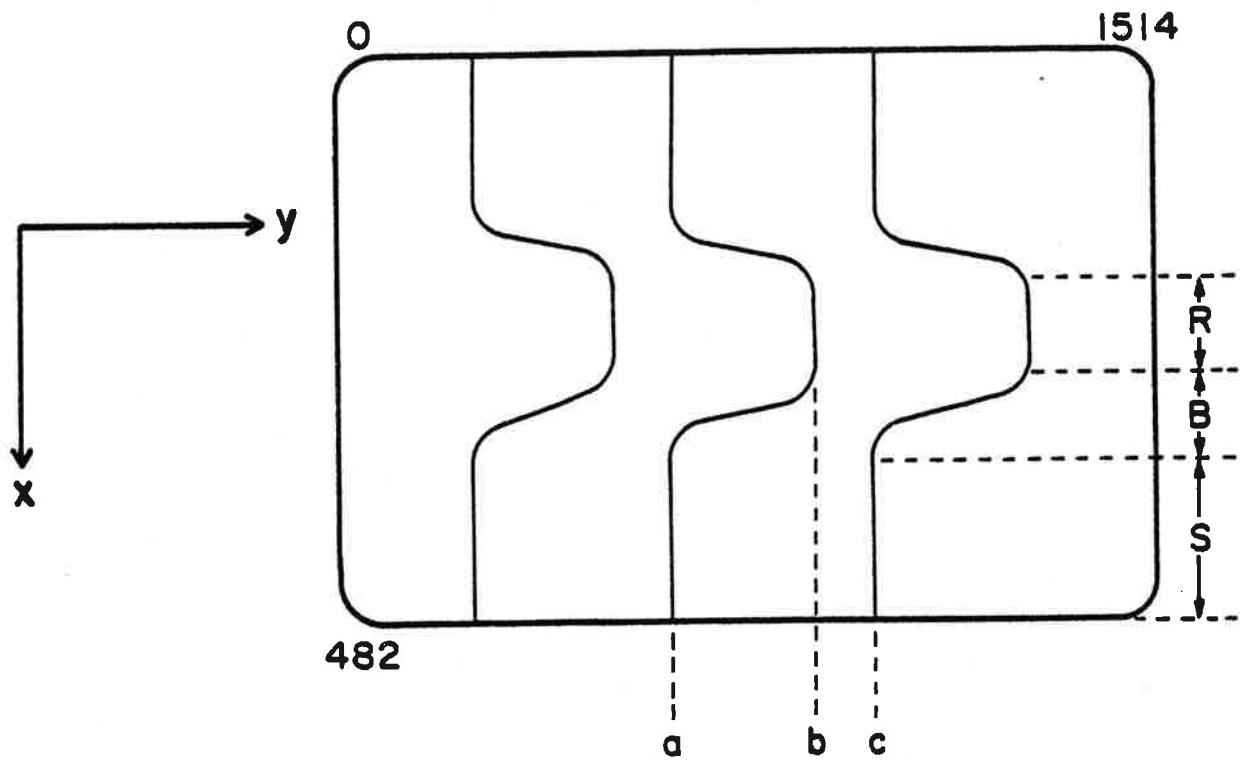


Figure 2.3 Schematic representation of the fringe shift,
 $N = ab/ac$.

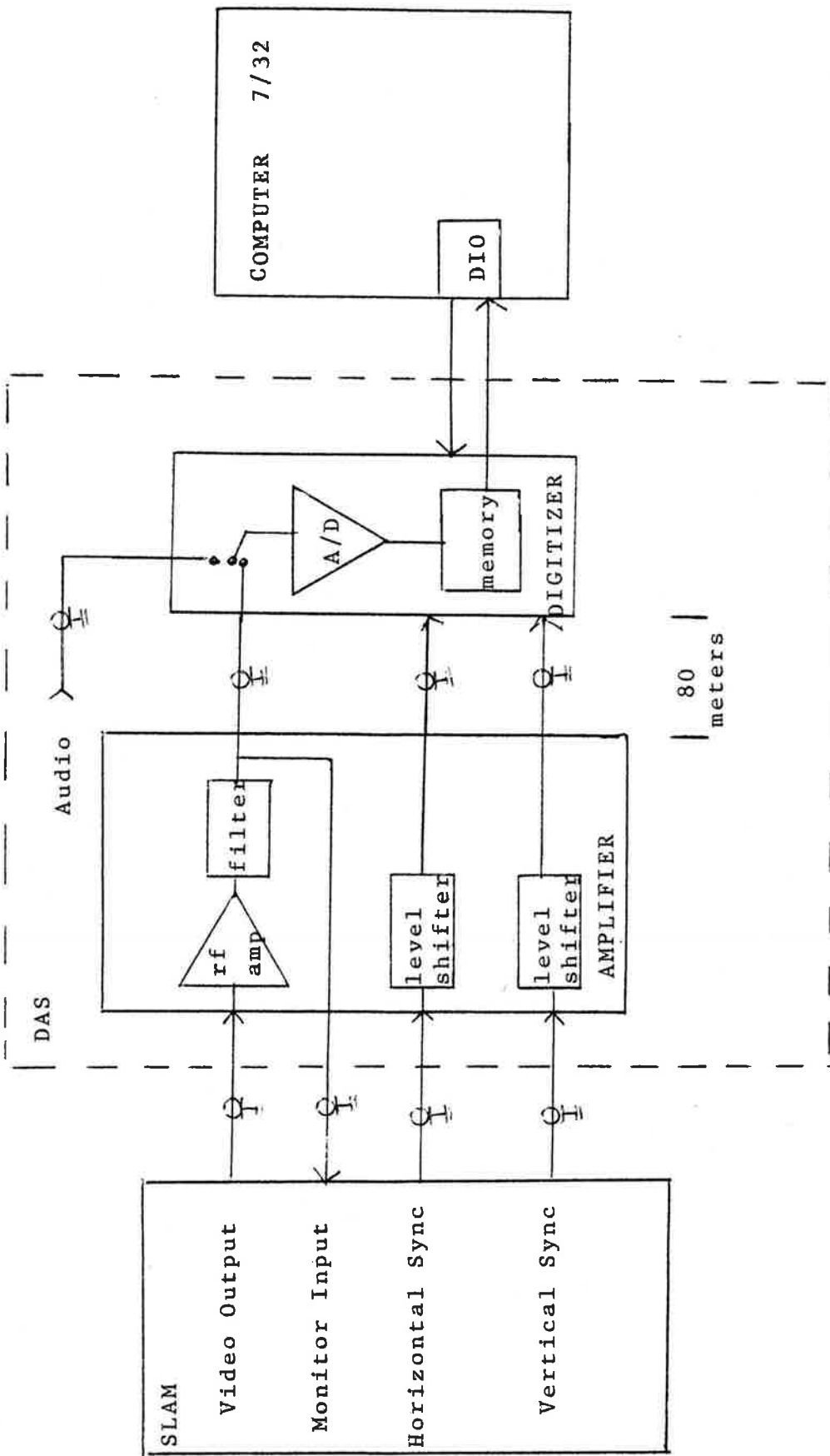


Figure 2.4 Block diagram of DAS.

The A/D and the buffer memory are collectively called the digitizer and are local to the computer. The rf amplifier is local to the microscope, 80 meters from the computer. The input range of the A/D is ± 500 mV which is monitored by an oscilloscope to assure that the entire voltage range is utilized for the best resolution of the A/D.

One raster line (of which there are a total of 482) at a time is digitized and stored in the buffer memory (1024 x 16 bits, 35 ns access time). Following the A/D conversion of an entire line (1514 points), the data are transferred into the computer memory. This operation is repeated for all 482 lines.

Included in the DAS project were the development of two programs which provided the capability to create printouts of the digitized interference image and an enhanced interference image on the line printer. The first program digitizes the data, averages it n times (selectable between 1-16 times), stores the data on magnetic tape, and outputs an image very similar to that displayed on the television monitor onto the line printer. The averaging is done using a complicated running averaging algorithm which was developed to compensate for slight horizontal jitter of the microscope image. It has been shown (Foster, 1981) that by increasing n , the quality of the resulting image is improved by minimizing of unwanted jitter-type noise which was evident on the interference lines (Figure 2.5) with the trade-off that the total digitization time is increased. A single sample takes approximately 30

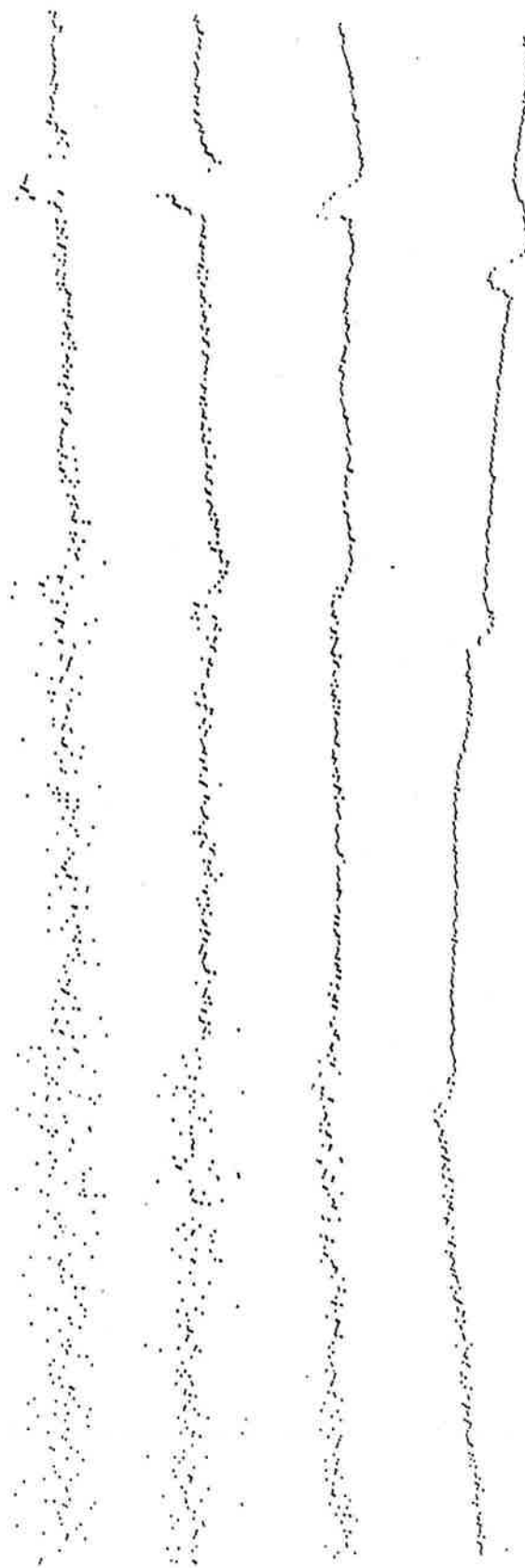


Figure 2.5 Effects of averaging on interference lines, from left to right the average is 1, 4, 16, and 64.

minutes to completely analyze for $n = 4$. For $n = 8$, sample analysis time is increased to 40 minutes and for larger n , significantly longer. Thus for only 3 samples, the time required for $n = 8$ is 30 minutes longer than for $n = 4$. Therefore, n was chosen to be 4, mainly due to time constraints. As it is important to maintain in vivo conditions, examining the specimens as soon as possible is necessary.

The second program enhances the interference image. A correlated receiver compares the waveform of each raster line to that of an ideal waveform stored in memory, detects a relative maximum in the correlated result and defines the interference line. The enhanced interference image consists of lines of only one data point in width, with each raster line now consisting of only 39 points. A quick comparison of Figures 2.1 a and 2.1 b illustrates this difference. This technique utilizes the full dynamic range of the digitized video signal.

2.3 THE FILTER

Enhancement of the interference image is obtained by using a bandpass filter with center frequency of 795 ± 2.5 kHz and a Q of 1.99 attached at the output of the rf amplifier (Figure 2.4). This filter eliminates noise outside of its bandwidth. Since the video portion of the raster line is 52.5 microseconds and this portion of each raster line consists of 39 interference lines, the average time period

between interference lines is 1.35 microseconds, or its average frequency is 740 kHz. Using a Q of 1.99 allows a sufficiently wide bandwidth to pass valid data and eliminate a substantial amount of the noise. Figure 2.6 illustrates the filter's effect using a liver sample that was processed with and without the filter and digitized. The photographs reveal that the filtered image is not as fuzzy as the non-filtered image. The correlated interference printouts (Figure 2.6) show that for any interference line in 2.6 c and the corresponding interference line in 2.6 d, it can be seen that the interference line varies less, i.e., it is not as noisy as the unfiltered line.

2.4 CALCULATION OF THE SPEED OF SOUND USING AUTOMATED PROGRAM

Previously, the speed of sound in a specimen has been determined manually by drawing in the lines a, b, and c (see Figure 2.3) and then computing the distances ab and ac to calculate the normalized lateral fringe shift, $N = ab/ac$ (Goss and O'Brien, 1979). Typically this involved measuring these parameters at three different regions in a specimen and averaging the result. This particular method is subject to several judgements on the part of the operator. Specifically, as the lines are not completely linear, as can be seen in Figure 2.6 for example, "eye-balling" the best fit lines a, b, and c was necessary. Also, the operator had to choose points from which to measure the distances ab and ac. The computer program(see appendix) that has been developed eliminates the need to do this manually, increases the area

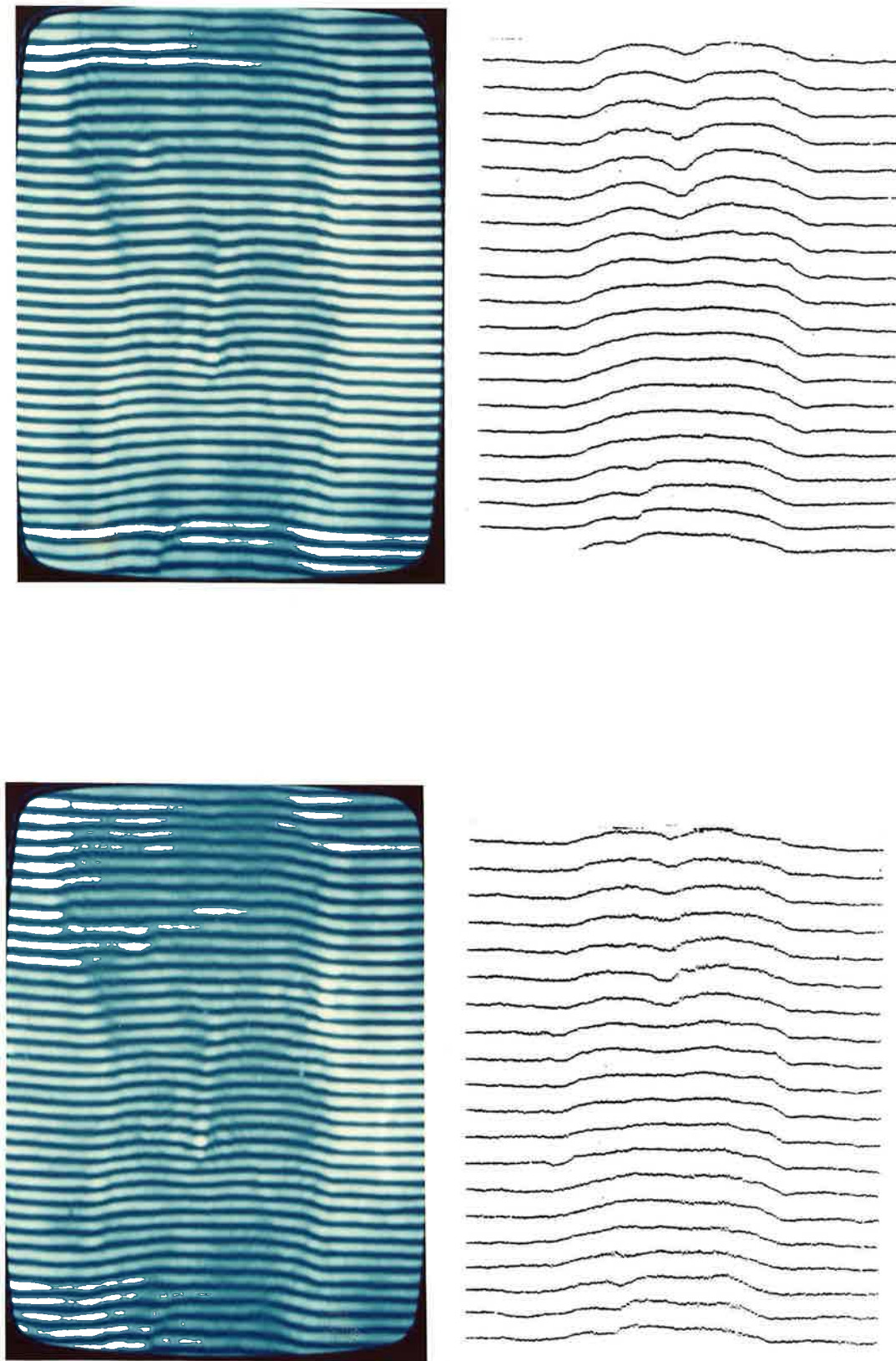


Figure 2.6 (clockwise from top left) a) photograph of liver sample as displayed on television monitor without filtering b) photograph of liver sample as displayed on television monitor after filtering c) correlated interference image of the left half of (b) d) correlated interference image of left half of (a).

of tissue for which the speed can be calculated, and involves minimal operator interaction.

Following digitization of the image and subsequent enhancement of the interference pattern, the interference lines are stored in memory in array form. A single interference line and the adjacent interference line provide the information necessary to determine lines a and b, and calculate the distances ab and ac provided the specimen is placed within the boundaries $x = 51$ to $x = 432$ as shown in Figure 2.3. The reason for this requirement will be explained shortly. The array for a single interference line consists of 482 data points. The top and bottom 50 points (100 total) are always used to determine line a, which is characteristic of the reference medium not a specimen, hence the specimen must lie within the two boundaries. The best fit straight lines a and c are found using a least squares, linear approximation given by

$$b = \frac{\sum(x_j - \bar{x})y_j}{\sum(x_j - \bar{x})^2} \quad (3)$$

$$y_j^1 - \bar{y} = b(x_j - \bar{x}) \quad (4)$$

where \bar{y} is the average value of y which can range from 0 to 1514, \bar{x} is the average value of x (for 482 points per line, the average is 241.5), x_j 's are the values 1-50 and 433-482, and the y_j 's are the values of the array for the

corresponding x_j values. Similarly, this procedure is repeated on the array containing the information of the interference line directly adjacent and to the right of the of the initial interference lines. Once lines a and c are defined, the distance ac is calculated for each point $x = 1 - 50$ and $x = 433 - 482$ and the average ac determined. It is this average value of ac which is used for the remainder of the calculations of the speed for that specimen.

As mentioned earlier, the array of the interference line contains the data necessary to compute ab for a specified region R (see Figure 2.3), i.e., the region which has the fringe shift data for the specimen being examined. This region R, over which the distance ab will be calculated, is a variable that the operator inputs to the program. The rationale for this is that not all the data in the regions $x = 51 - 432$ may actually be useful specimen data because 1) the specimen may not take up the entire region R, 2) the specimen may not be uniformly thick over the region due to edge effect, 3) it may be necessary to avoid certain inhomogeneities in the tissues, such as blood vessels. Following input of the region R the distance ab will be calculated R times. N is now determined using each ab and the average ac previously calculated for that specimen. Given the sample thickness, the speed of sound data set (R total values) is determined.

In addition various statistical parameters can be

calculated from each speed of sound data set, namely the standard deviation, mean, mode, and median, and the skewness and kurtosis of the distribution of the speeds. In order to fully discuss these parameters, their derivation and significance, a short discussion of moments is necessary. This information has been derived from Spiegel(1961).

The rth moment is defined as

$$x^r = \frac{1}{N} \sum_{j=1}^N (x_j)^r \quad (5)$$

which for $r = 1$, is recognizable as the mean. It is about the mean that several other quantities are defined. The rth moment about the mean

$$m_r = \frac{1}{N} \sum_{j=1}^N (x_j - \bar{x})^r \quad (6)$$

is an indication of the properties of a particular distribution. It is sometimes desirable to use a dimensionless moment about the mean and is defined

$$a_r = \frac{m_r}{s^r} \quad (7)$$

where s , the standard deviation is defined as

$$s = \sqrt{\frac{1}{N} \sum_{j=1}^N (x_j - \bar{x})^2} = \sqrt{m_2} \quad (8)$$

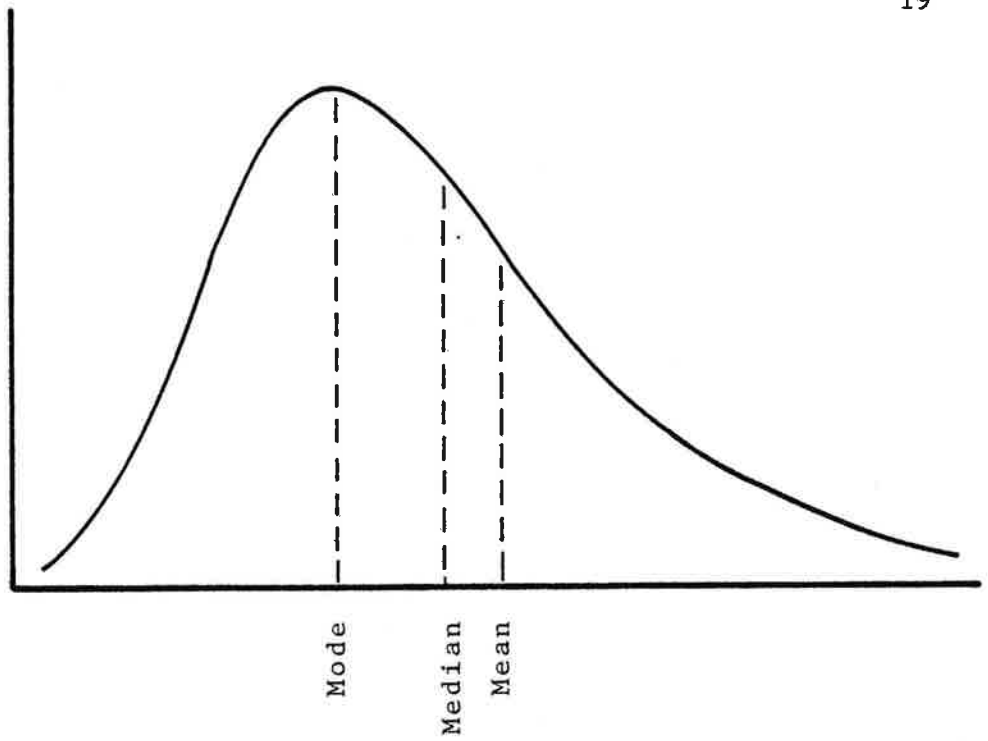
where \bar{x} is the mean value, N is the number of samples, and x_j

is the j th value. In the determination of the standard deviation of the speed \bar{x} is the mean speed, x_j is the j th speed value along the region R , where R consists of the number of samples. The standard deviation is used to measure the concentration of values around the mean. As the data base is more spread out from the mean, the standard deviation will increase.

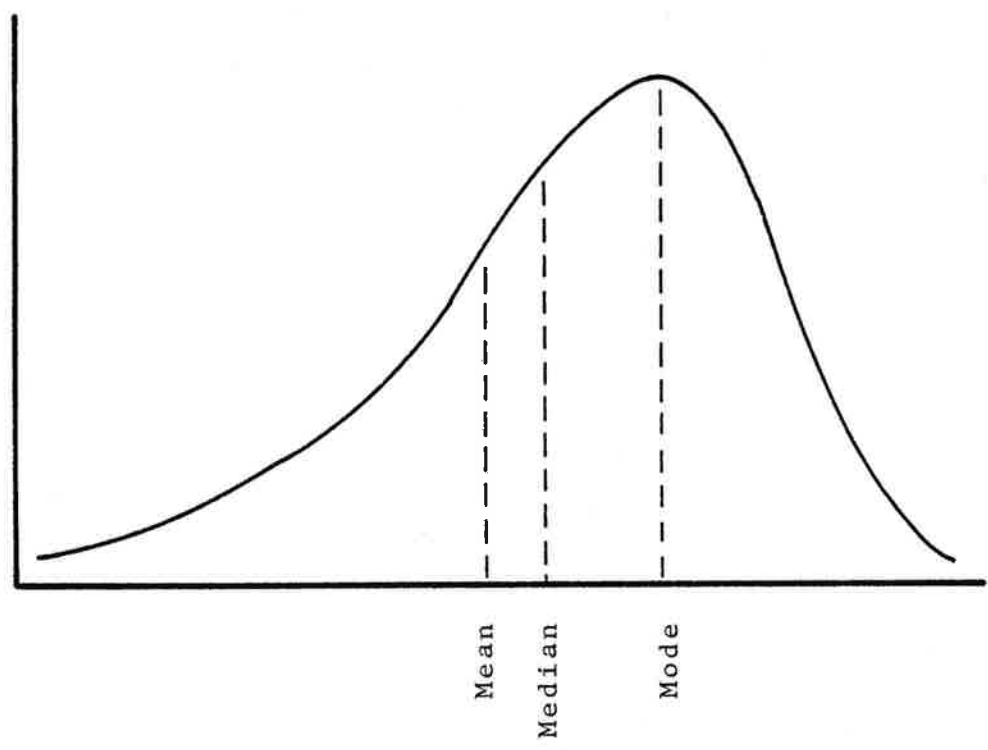
The mode is that value which occurs more frequently than any other value; graphically it appears as the peak of a distribution (see Figure 2.7). The mode may not exist or also may not be unique (e.g., bimodal and trimodal distributions). In this project, the mode represents which speed of sound value that is the most prevalent.

Of a set of numbers arranged in order of magnitude, the median is the value of the exact middle position of that set (see Figure 2.7). If P indicates the number of values and P is odd, then the median is the value of the position defined by $(P + 1)/2$. For example, of the set (4, 5, 6), $P = 3$ and $(P + 1)/2 = 2$, therefore the median is 5. In this particular program, P is always chosen to be odd, therefore only one algorithm is needed, P even need not be considered. The reader can refer to Spiegel(1961) for a discussion of P even. Within the program the computed acoustic speeds are arranged in magnitude order and the median value identified.

Skewness is an indication of the "sidedness" of a distribution with respect to its mean.



a) Positive (right) skewness



b) Negative (left) skewness

Figure 2.7 Skewness curves.

By definition

$$\text{skew} = \frac{\bar{x} - \text{mode}}{s} \quad (9)$$

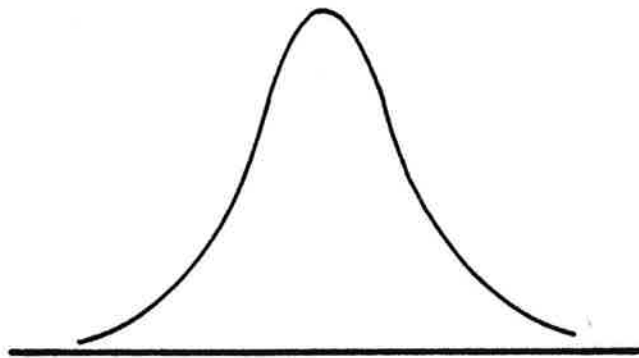
If more of the values of a distribution are to the right of the mean, the distribution is said to be right skewed or positive, i.e., by using Figure 2.7 a as a guide, the quantity $(\bar{x} - \text{mode})$ of equation (9) will be positive under these conditions. Alternatively if more of the distribution is to the left of its mean, the distribution is said to be left skewed or negative, i.e., the quantity $(\bar{x} - \text{mode})$ is negative (see Figure 2.7 b). Consider the case of a perfectly straight interference line, such as that shown in Figure 2.3 region R. The distribution of the speed data set would be a single line at a speed Cx . In this case the mean and mode are equal, and the skew is identically zero. However, a perfectly straight interference line is not typical, rather the lines vary such as those in Figure 2.6. Therefore, the quantity $(\bar{x} - \text{mode})$ will rarely be identically zero. This result can be attributed to the heterogeneity of the specimen, the resolution of the digitizer and the non-uniformity of the sound field. Thus, positive or negative skewness is not as important as the degree of skewness.

Kurtosis, another measure of the shape of a distribution, reveals the degree of peakedness of that distribution as compared to a normal distribution. Curves fitting the definitions of leptokurtosis (spikey, very

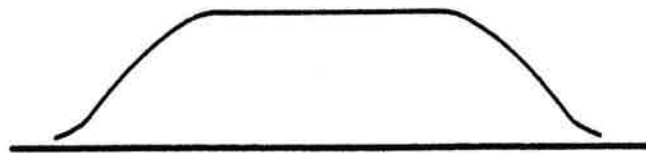
peaked), platykurtosis (flat) and mesokurtic (normal) are shown in Figure 2.8. The kurtosis is defined by the 4th moment around the mean; in this case a dimensionless form is used, namely

$$a_4 = \frac{m_4}{s^4} \quad (10)$$

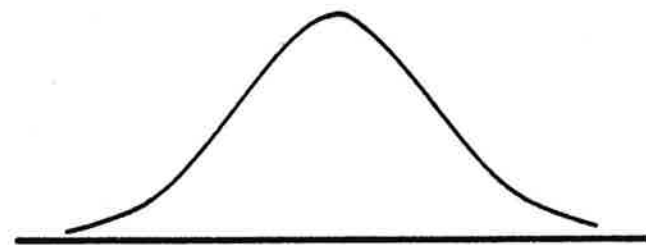
For normal (or Gaussian) distributions (mesokurtic) a_4 is defined to be equal to 0, thus a distribution is said to be leptokurtic for $a_4 > 0$ and platykurtic for $a_4 < 0$. As in the case of the skewness, an absolute number is not the factor that is in question, rather the degree to which the distribution is normal. If the values of the kurtosis are within some set limits, then it can be concluded that the distribution is normal and any of the assumptions that have been made regarding normality are indeed true.



a) Leptokurtic



b) Platykurtic



c) Mesokurtic (normal)

Figure 2.8 Kurtosis distributions .

CHAPTER 3

METHODS OF PREPARATION

3.1 SPECIMEN PREPARATION

White, ICR female mice (Harlan Sprague Dawley strain) approximately 6-7 months old were sacrificed by means of spinal cord dislocation so as to not introduce any drugs into the tissues of the mice. Liver or spleen was quickly excised (within 5 minutes post mortem) and immediately placed in isotonic saline solution. As this experiment is a lengthy one, only one tissue type was used from a single animal to insure freshness. All tissues were examined within 90 minutes of sacrifice.

The tissue was cut into sections ranging from 400 - 800 micrometers, specifically 460, 610, and 760 micrometers with the guillotine-type device shown in Figure 3.1. The guillotine operates by releasing the razor blade arm down upon a sample on the stage, slicing off a section of thickness T . By moving the micrometer, any thickness desired can be measured and cut. The guillotine was used for several reasons: 1) fresh specimens could be used, 2) specimens of a desired thickness could be obtained, 3) the compression of the tissue and therefore one consideration in the measure of the accuracy of the thickness has been shown to be minimal (Teyler, 1980), and 4) it is relatively easy and quick to use.

Originally, frozen sections were prepared with a Lipshaw

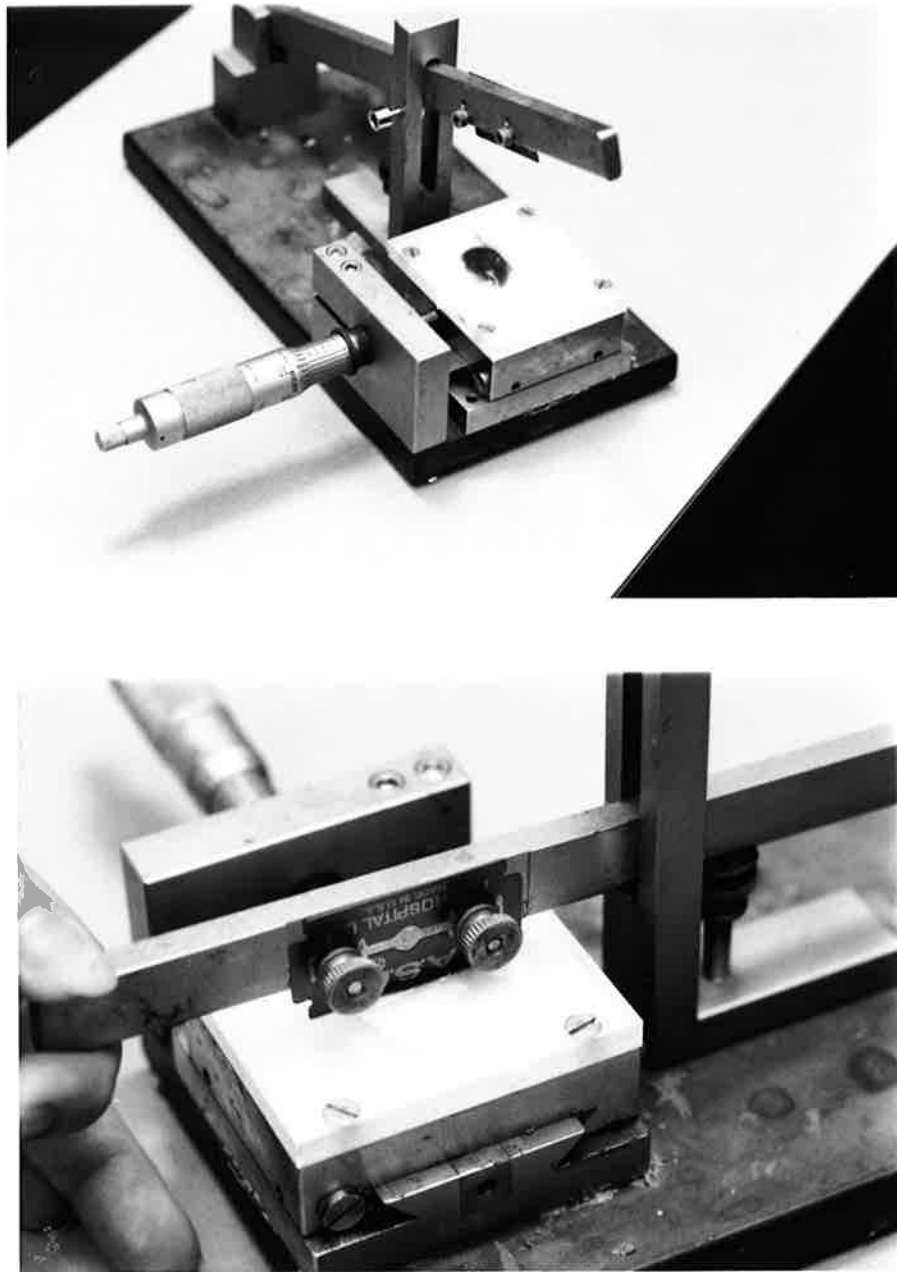


Figure 3.1 Guillotine-type device used to cut sample thicknesses.

cryostat microtome (Cryotome), but this proved to be unsuccessful. Although the cryotome was ideal for cutting specimens to thicknesses of less than 400 micrometers, thicker specimens tended to fracture. The Cryotome required that the tissue be frozen which meant more handling of the tissue and yielding a specimen a further step removed from the in vivo situations.

The guillotine is not without its problems. Special care had to be taken to keep the specimen stationary from slice to slice. Filter paper, wetted with saline solution, does hold the sample stationary, but can slide around if too much saline solution is added. Also to insure cutting of accurate thicknesses, the guillotine should be zeroed before each slice as the tissue will shrink away from the previously cut edge if allowed to sit too long. Zeroing is simply done by cutting off a small slice immediately before cutting a sample for the microscope.

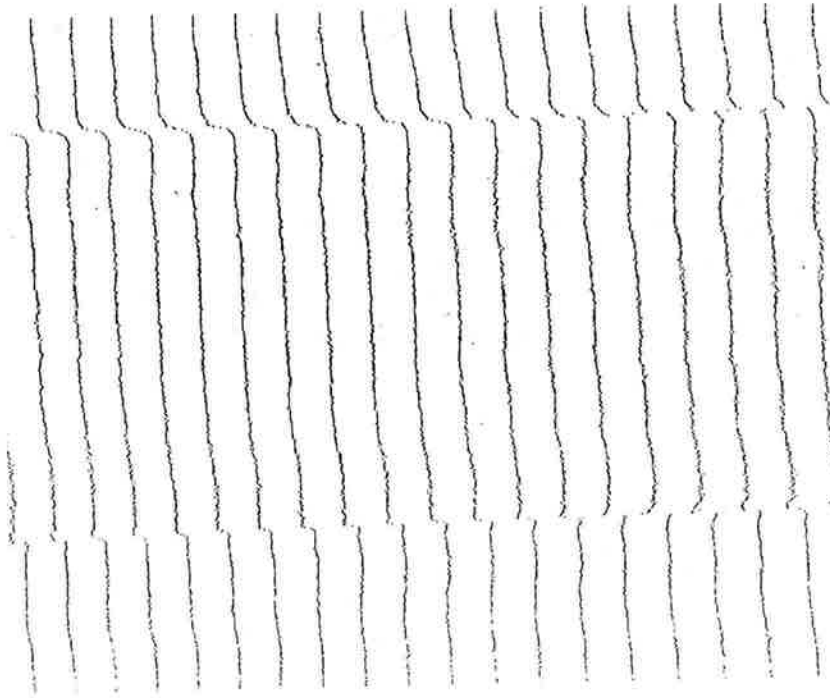
The thicknesses used, 460, 610, and 760 micrometers, were chosen for several important reasons. 1) When using the guillotine, there was a practical limit as to how accurate thinner specimens could be cut. Thicknesses of 450 micrometers worked best. 2) An upper limit existed of how thick a specimen can be used with the SLAM. Thick specimens can be very attenuating making it difficult to produce a usable interference image.

The sample is then trimmed with a razor blade into a rectangular piece appropriately suitable in size for viewing

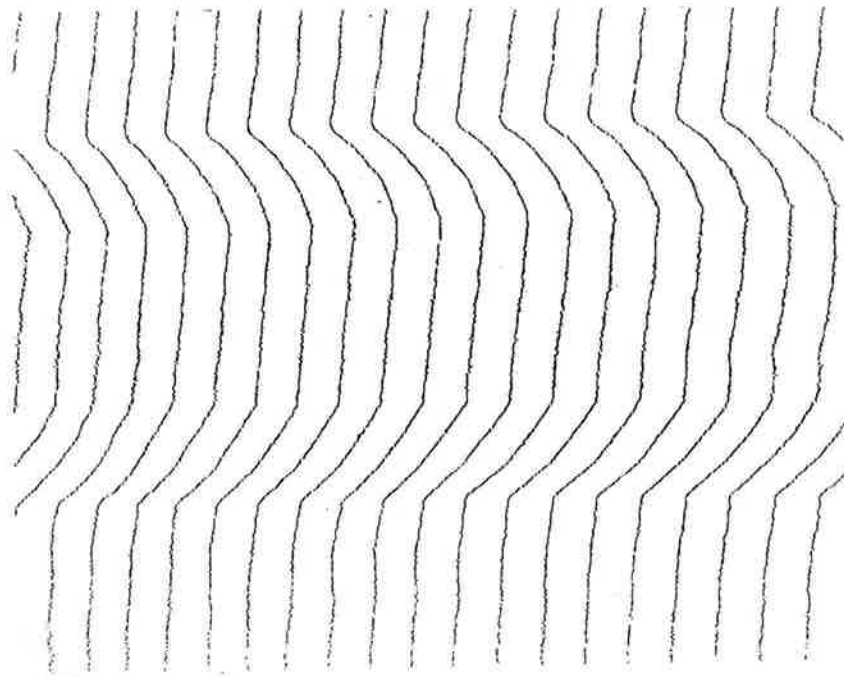
with the SLAM. Recall that the field of view is approximately 3 mm x 2 mm, and that the speed of sound can only be determined if there is no discontinuity of the interference line between the saline and tissue and thus, the edges of the specimen are bevelled(see Figure 3.2 a). With such a discontinuity, the computer program as currently written fails as it requires reasonably continuous interference lines. Even the manual procedure might yield false results. Beveling the edges and subsequent digitization shows where the actual fringe shift is in a particular specimen, quite different than the non-bevelled image reveals (see Figure 3.2 b).

3.2 MICROSCOPE PREPARATION

The SLAM must also be prepared for sample investigation. The microscope slide(see Figure 3.3) is 9 cm square with a 6 cm diameter center. It is in this center that a metal ring(6 cm outside diameter) fits, securing a very thin plastic sheet between it and the plastic square. The slide is acoustically coupled to the top surface of the fused silica stage using a few drops of distilled water. The microscope slide is used to prevent scratching of the stage and also to aid in the positioning of the specimen within the sound field. The sample is then placed in the center of the slide, on the plastic sheet, and surrounded by a spacer which has a thickness slightly greater than the sample. The spacer prevents the sample from being crushed or distorted by the



a) plastic sample without bevelled edges



b) plastic sample with bevelled edges

Figure 3.2 Illustration of the effect of bevelling sample edges.



a) Microscope stage



b) close-up of stage with microscope slide in position on top



c) close-up of spacer and coverslip on the microscope slide

Figure 3.3 Photographs of microscope stage

coverslip, insures a constant distance between the slide and the coverslip, and keeps the coverslip level with respect to the stage. The area surrounding the tissue is filled with saline, which serves as the reference media, to keep it fresh.

The coverslip (Figure 3.3) is a partially mirrored lucite block that rests over the specimen, supported by the spacer. It is this mirrored surface from which the laser light is reflected that has been modulated by the mechanical perturbations introduced to the sample by the 100 MHz transducer beneath the stage, to the acoustic image detector. An optical image of the sample is provided as the coverslip does allow light to pass through to the optical detector in the base of the stage (see Figure 3.4). Some specimens, such as metal are optically reflective, would not require use of the coverslip. Biological specimens, however, do as they are not naturally reflective.

Once the sample is under the microscope, the stage is adjusted in three dimensions to achieve optimal focusing of the laser beam, bearing in mind that the interference lines must be reasonably continuous.

3.3 DATA COLLECTION

Data collection consists of running both a master program and the speed program. The master program consists of several smaller programs, namely the digitization and interference programs from the DAS project. Thus the program

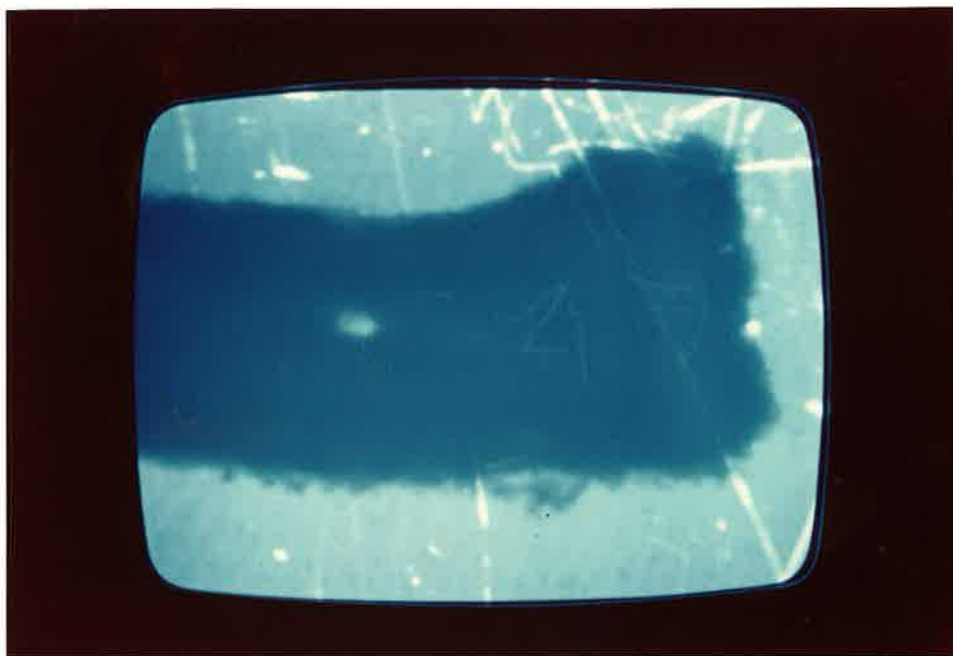


Figure 3.4 Optical image of liver sample as produced by the SLAM.

will digitize the image, store it on tape, run the correlation program and output both the interference image and the enhanced interference image onto the line printer. This program requires a title (identification purposes) and the number of averages to be done and it runs without further operator input for approximately 15 minutes. Specifics regarding the master program can be found in Foster (1981).

Immediately following the master program, the speed program is run. The operator inputs the interference line required (one of the 39 available), the thickness of the specimen, a title, and the region R. This program takes approximately 3 minutes.

Typically, the speed is calculated for 3 different lines of the interference image, usually lines 15, 20 and 25. These particular interference lines are in the middle of the sound field. R ranges from 60 - 120 points, and is chosen by the operator. The speed program will output all the statistical parameters previously mentioned, a graphical distribution of the speeds, and the interference line being used with the area R imposed on it (see Figure 3.5).

Following each sample, the saline solution is changed as particles tend to suspend themselves and will disturb the sound beams. After each tissue type is completed, the plastic sheet of the microscope slide is replaced, as any flaws can also disturb the propagation of the sound through it. Occasionally the coverslip is replaced as the gold mirroring will scratch off, and if there is no mirroring

```
NUMBER OF AVERAGES= 4
LINE#   SLOPE   YBAR   XBAR
 25     -0.01   907.14 241.50
LINE#   SLOPE   YBAR   XBAR
 26     -0.01   946.35 241.50
NS=180  NE=300  N=121
THICKNESS(M) = 0.00054
VMIN(M/S)= 1559.023  VMAX(M/S)= 1568.172
AVERAGE SPEED(M/S)= 1564.564  STANDARD DEVIATION(M/S) = 2.270
LEPTOKURTIC      5.35
MEDIAN SPEED(M/S)= 1564.239
SKEWED RIGHT     0.430
MODE OCCURS AT 1564M/S  VALUE OF 28.00
```

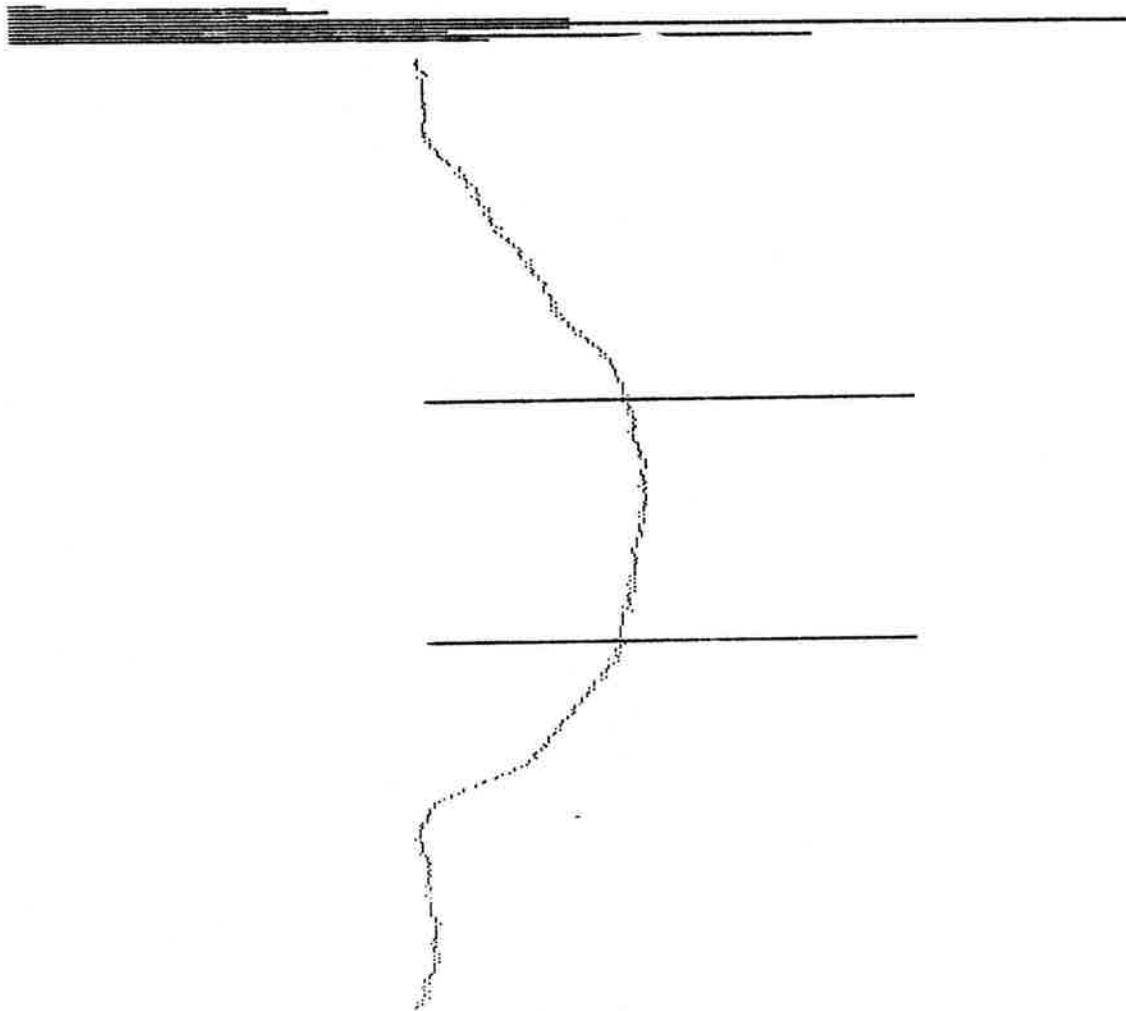


Figure 3.5 Typical data sheet that is obtained after running the speed program.

there is no reflection, hence the laser beam is unable to detect the mechanical perturbations of the tissue.

CHAPTER 4
ERROR ANALYSIS

The sources of error which are considered in the determination of acoustic speed include 1) the measurement of N , 2) the sample thickness, and 3) the use of the bandpass filter.

The normalized fringe shift, N , is defined by:

$$N = \frac{ab}{ac} \quad (11)$$

where ac and ab are described in Figure 2.3. Let us consider the expression

$$N = \frac{ab + \Delta ab}{ac + \Delta ac} \quad (12)$$

where Δac and Δab represent the inaccuracy in measuring ac and ab , respectively. Multiplying both numerator and denominator by $ac - \Delta ac$ is

$$N = \frac{ab \cdot ac + \Delta ab \cdot ac - ab \cdot \Delta ac - \Delta ab \Delta ac}{(ac)^2 - (\Delta ac)^2} \quad (13)$$

Making the assumption that Δac and Δab are sufficiently small so that the second order terms such as $(\Delta ac)^2$ can be ignored, equation (13) becomes

$$N = \frac{ab \cdot ac + \Delta ab \cdot ac - ab \cdot \Delta ac}{(ac)^2} \quad (14)$$

Rearranging the terms, N becomes

$$N = \frac{ab}{ac} \left[1 + \frac{\Delta ab}{ab} - \frac{\Delta ac}{ac} \right] \quad (15)$$

Under worse case assumptions whereby the two fractional terms in brackets contribute constructively to the error, one can define the percentage error by

$$\text{error}(N) = \left[\left| \frac{\Delta ab}{ab} \right| + \left| \frac{\Delta ac}{ac} \right| \right] \times 100 \quad (16)$$

As saline is used as the reference medium, the distance ac is typically 39 points wide (1514 points, 39 lines evenly spaced across). The inaccuracy of measuring both ab and ac is ± 0.5 point. Therefore $\Delta ac/ac = \pm 1.28\%$. The distance ab changes with increasing thickness. For a thin specimen, 460 micrometers ab is approximately 31 points and $\Delta ab/ab = \pm 1.6\%$. The total error of N is $\pm 2.9\%$. For a thick specimen, 760 micrometers, ab = 78 points, thus $\Delta ab/ab = \pm 0.6\%$. The total error in N is $\pm 1.9\%$.

To analyze the uncertainty of the specimen thickness, samples were cut and then measured using an independent measuring technique. Using a micrometer of accuracy ± 0.02 mm, three samples of each of the three thicknesses for each tissue type were examined. Following analysis of the data, the accuracy of the thicknesses is essentially the same for both liver and spleen, specifically 460 ± 25 microns (5.5% error), 610 ± 25 microns (4.1% error) and 760 ± 13 microns

(1.7% error).

The effects of N and T uncertainty on the acoustic speed calculations is best illustrated by example. Consider the case where $T = 460$ micrometers and $N = 1.054$ and $C_x = 1560$ m/s. Varying either N or T and keeping the other parameter constant for this case will give an indication of the independent effect of each in the speed calculation, although N and T are not independent. The $\pm 5.5\%$ uncertainty in T for 460 yields a variation in C_x of $\pm 0.2\%$ while the 2.9% uncertainty in N for 1.056 yields a variation in C_x of $\pm 0.1\%$. It appears that C_x is more affected by the 5.5% uncertainty in T, than the 2.9% uncertainty in N. This is not a surprising result as the uncertainty of T is greater than the uncertainty of N.

A thicker specimen has a different uncertainty, therefore it is necessary to do an analysis for thick specimens also. Consider the case where $T = 760$ micrometers, $N = 1.741$ and $C_x = 1560$ m/s. The $\pm 1.7\%$ uncertainty in T for 760 micrometers yields a variation in C_x of $\pm 0.06\%$ and the $\pm 1.9\%$ uncertainty in N for 1.741 yields a variation in C_x of $\pm 0.06\%$. For thick specimens the uncertainty in measuring either N or T is almost equal, thus the effect on C_x is approximately the same.

The limiting cases of accurately determining C_x will occur when the ratio of N/T as used in equation (1) is maximized or minimized. Using the same values for T and N as used previously and incorporating their respective

uncertainties to calculate the maximum and minimum N/T, the following values for Cx result

<u>T</u>	<u>N</u>	<u>Cx</u>		
435	1.084	1564.8	}	± .3%
485	1.023	1555.6		
747	1.774	1562.0	}	± .16%
783	1.708	1557.4		

Thus the uncertainty in the speed calculation for thin specimens is $\pm 0.3\%$ and for thick specimens $\pm 0.16\%$. The percentages may seem insignificant, but $\pm 0.3\%$ is ± 5 m/s and $\pm 0.16\%$ is ± 2.5 m/s when using 1560 m/s as the relative number. If two different specimens are being examined, this inaccuracy might be significant if the specimens have speeds that are fairly similar (e.g., ± 5 m/s). It would be impossible to distinguish them apart on this basis alone. As the inaccuracy decreases as the thickness increases, one might think to use a thick sample. For a very highly attenuating specimen, however, it may be difficult to produce a sample suitable for use with the SLAM due to the fact that the detected acoustic signal may be outside the dynamic range of the SLAM.

The step response of the filter and rf amplifier is shown in Figure 4.1. Only one cycle later, the response has decayed to less than 20%. Thus, as the raster line is filtered, 20% of the previous waveform is added to the next waveform. As long as raster line is periodic with the same frequency, this additive effect will not significantly change

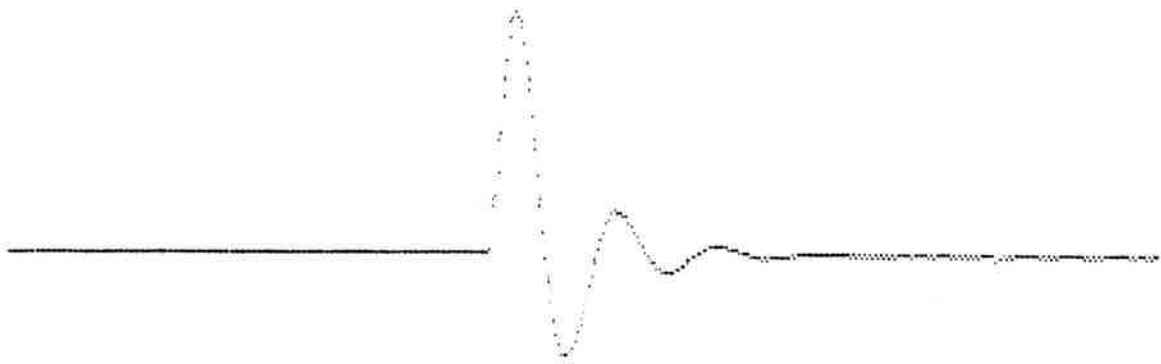
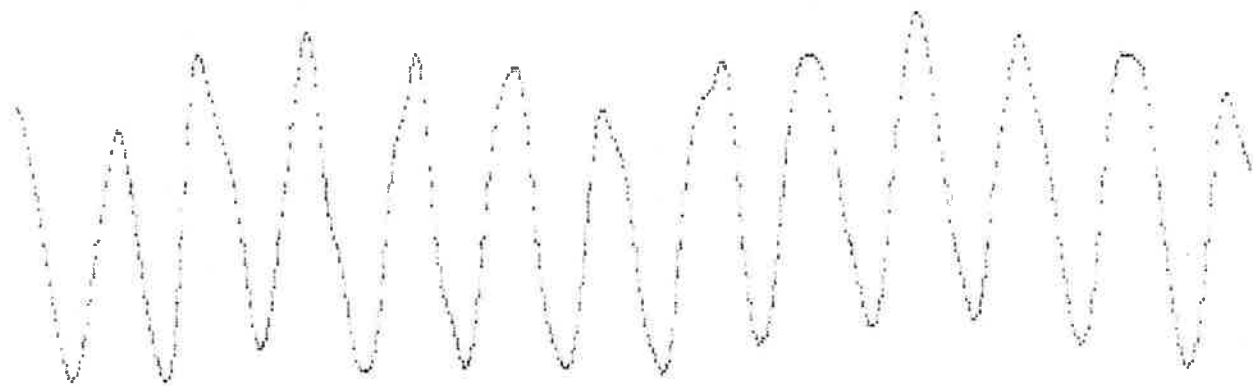


Figure 4.1 Step response of the bandpass filter.

or distort the data. Such is the case of a field of only one material, e.g., saline. A typical raster line is shown in Figure 4.2 a. After filtering this raster line, Figure 4.2 b shows that the raster line has not been distorted, but the noise has been minimized. However, this response may be important when the raster line is not periodic for its entire length, such as the case of the interface between the reference medium and a specimen. An abrupt phase shift will distort the raster line, making it no longer periodic (Figure 4.3 a). If then filtered the raster line may be further distorted for that region because of the non-periodic additive effect of the filter (Figure 4.3 b). However, because of damping, the effects of the response to the previous point will be negligible 2-3 cycles later. Once again when the raster line is periodic, the phase shift will be minimal from point to point as described for the saline only case. The filter will now only eliminate noise. This problem may be avoided by not using an interference line in the vicinity of the interface to compute the speed.



a) raster line for saline only without filtering



b) raster line for saline only with filtering

Figure 4.2 The effect of filtering for the saline only case.

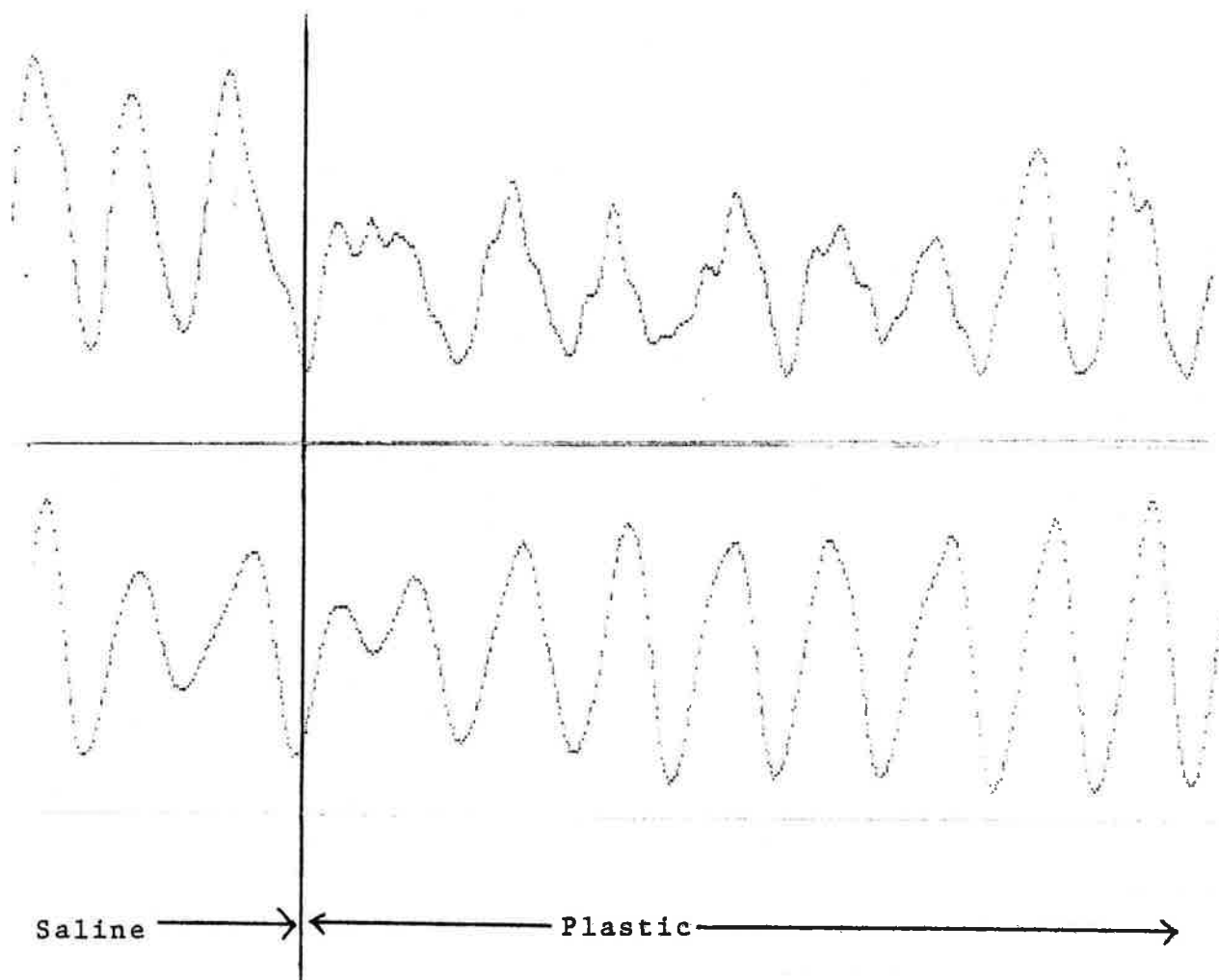


Figure 4.3 The effect of filtering for saline-plastic interface

- a) (upper) raster line for saline-plastic interface without filtering
- b) (lower) raster line for saline-plastic interface after filtering.

CHAPTER 5

RESULTS AND DISCUSSION

In Table 1, the data obtained in the project is tabulated, namely the sample type, number and thickness, the interference line used, the number of data points, the average speed of sound value, the standard deviation of the speed, the skewness and the kurtosis.

Although it was stated earlier that interference lines 15, 20 and 25 were used to compile data, other lines were used if these lines were not continuous or if it were necessary to avoid an inhomogeneity such as a blood vessel.

The average speed of sound value in Table 1 represents the average value for a single interference line for R data points. The average of the average values is 1556.3 m/s for mouse liver and 1565.0 m/s for mouse spleen. These results are comparable to those cited in the literature for similar tissues using the SLAM. Frizzell and Gindorf (1981) obtained values of 1565 ± 7.8 m/s for sheep liver and 1567 ± 13.2 m/s for cat liver.

The average of the standard deviation values is ± 2.1 for liver and ± 3.2 for spleen. An average value, however, does not reveal some important factors, such as the degree of heterogeneity of a specimen. If a specimen is homogeneous, it would be expected that the standard deviation would be small, i.e., the speed of sound data set would be very closely centered around its mean. Alternatively, if a specimen is heterogeneous the standard deviation would be

Table 1 Liver and Spleen Data (61 data points for each sample)

Tissue Type & #	Thickness(μ)	Line #	Average Speed(m/s)	Standard Deviation(m/s)	Skew	Kurtosis
Spleen 1	460	15	1567.8	6.48	-0.76	-1.09
		22	1567.4	2.31	1.14	-0.55
		25	1565.5	4.24	1.26	-1.14
	610	15	1542.0	3.37	0.44	-1.13
		22	1563.6	5.80	-0.93	-0.23
		25	1564.8	5.24	-0.58	-1.52
760	19	1558.9	3.79	-0.26	-0.43	
	24	1561.5	3.44	0.86	-1.38	
Spleen 2	460	20	1565.1	4.93	-1.04	-1.17
		25	1572.1	2.20	0.66	-1.08
		19	1569.4	1.54	0.18	-0.87
	610	25	1568.2	1.94	-1.63	2.13
		15	1582.6	4.09	0.12	-0.67
		21	1570.9	4.00	1.07	-0.41
Spleen 3	460	15	1567.2	2.97	0.23	-0.59
		20	1575.0	4.93	0.07	0.08
		25	1566.8	2.13	-0.15	0.55
	610	17	1576.8	1.57	-0.22	-0.45
		20	1573.2	2.96	-0.58	0.48
		25	1554.3	1.97	-0.44	0.13

760* Data unavailable

Table 1 continued

Tissue Type & #	Thickness(μ)	Line #	Average Speed(m/s)	Standard Deviation(m/s)	Skew	Kurtosis	
Spleen 4	460	15	1574.5	3.84	-0.37	2.41	
		21	1575.2	3.85	-1.16	-0.69	
	25	1565.2	1.54	0.00	0.96		
	610	15	1551.2	1.07	0.71	0.85	
		21	1551.6	3.29	0.25	-1.24	
	760	25	1543.9	1.34	-0.14	-0.05	
15		1559.6	1.93	-0.14	-0.87		
20		1563.2	2.71	0.05	-1.25		
26		1568.1	1.98	-1.03	-0.31		
Liver 1	460	16	1563.8	1.68	0.25	-0.64	
		20	1564.0	1.26	0.41	0.85	
	25	1560.8	1.53	0.09	-0.05		
	610	15	1544.6	1.57	-0.06	-0.92	
		21	1553.4	2.84	-0.15	-1.34	
	760	25	1544.6	2.38	-0.49	0.65	
		14	1552.8	1.73	-0.43	-0.29	
	24	1552.1	1.58	0.44	-0.80		
	Liver 2	460	15	1555.4	3.32	-0.76	-1.40
			20	1556.0	3.09	-0.49	-0.56
25		1546.1	1.17	-0.17	-0.70		
610		15	1548.8	2.79	0.44	-0.84	
		20	1550.3	2.42	0.03	-0.63	
760		15	1567.9	2.23	-0.03	-0.60	
		20	1571.6	1.62	-0.02	-0.06	
25		1568.3	1.63	-1.10	-0.45		

larger. Recall that at a frequency of 100 MHz insertion loss can increase significantly with increasing thickness. It must be assumed that this insertion loss will affect the standard deviation of the speed of sound because of the decrease in the signal-to-noise ratio for thicker specimens; thus comparisons of specimens must be done for the same thickness only. Thus, if two different specimens of the same thickness are examined, the heterogeneity of one with respect to the other can be stated. In this project the standard deviation of spleen was generally greater than that of liver for all thicknesses. Thus, it is concluded that spleen is more heterogeneous than liver.

It should be noted however that the standard deviation did not increase with increasing thickness as originally thought. An examination of the relationship of N , the normalized lateral fringe shift, and T , the thickness of the specimen, does indicate a possible explanation. For specific values of C_x and T , the corresponding N was generated using a computer program. A graph of N vs. T is shown in Figure 5.1. Speed values of 1550, 1560 and 1570 m/s were chosen as they are comparable to the values obtained in this project and the thickness values used ranged from 100 - 1000 microns since the specimen thicknesses used fall within this range. Using a specific example:

	<u>T = 400</u>	<u>700</u>
$C_x = 1560$ m/s	$N = .917$	$N = 1.604$
$C_x = 1550$ m/s	$N = .749$	$N = 1.310$
$\Delta C_x = 10$ m/s	$\Delta N = .168$	$\Delta N = .294$

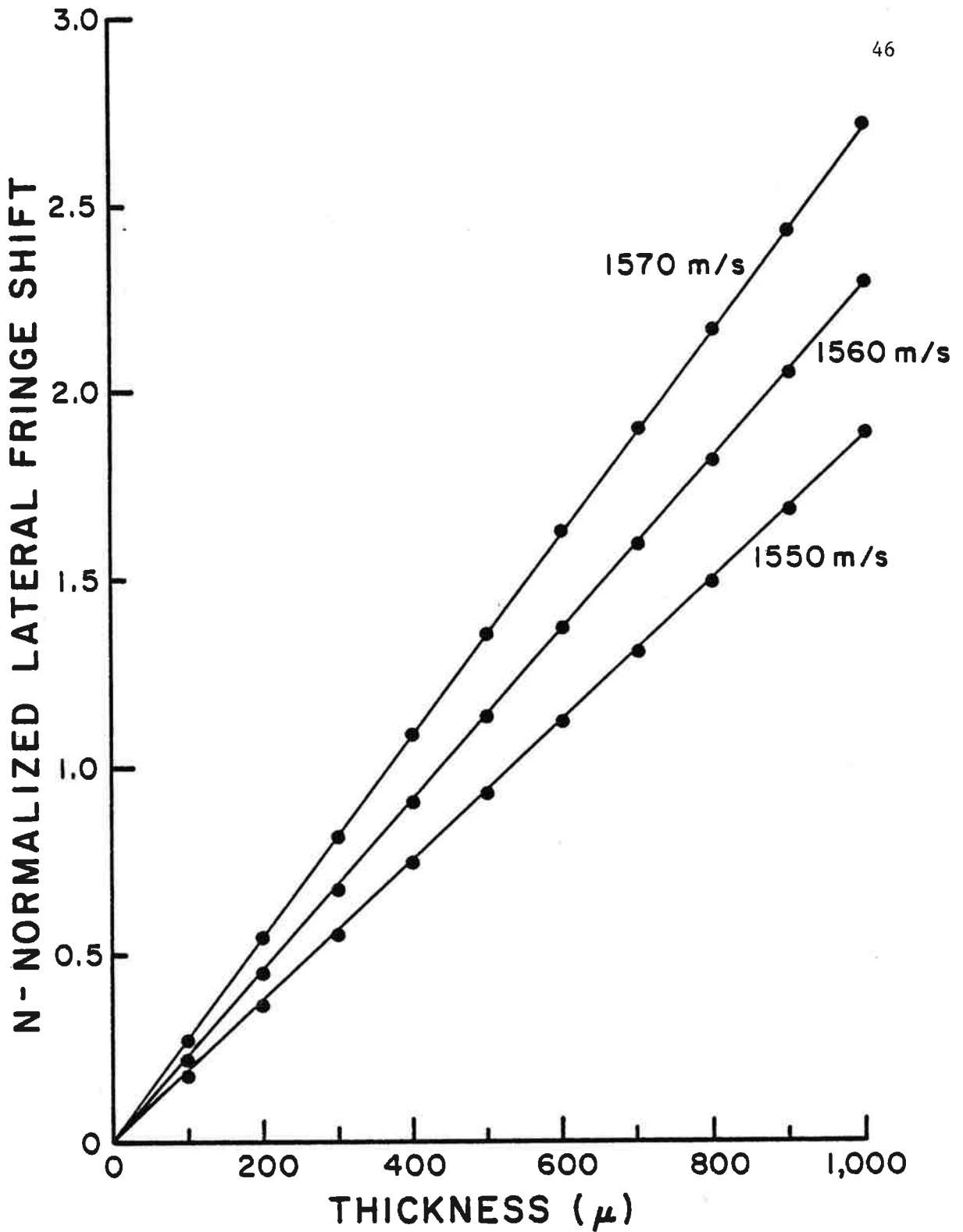


Figure 5.1 Graph of N vs. T (Table 2 lists specifics for this graph).

Table 2 Values of N vs. T graph as shown in Figure 5.1

T	Cx	1550	1560	1570
100		0.187	0.229	0.271
200		0.374	0.458	0.542
300		0.561	0.688	0.812
400		0.749	0.917	1.083
500		0.936	1.146	1.354
600		1.123	1.375	1.625
700		1.310	1.604	1.895
800		1.497	1.834	2.166
900		1.684	2.063	2.437
1000		1.871	2.292	2.708

The implications of this are that to effect a 10 m/s change at 700 microns requires a change in N of .294, while a change of 10 m/s at 400 microns requires a change in N of only .168. Thus the same change in N will affect the speed calculation differently at different thicknesses. Very thin specimens are more sensitive to variations in N.

Similarly, the same evaluation can be done for the thickness.

	<u>N = .75</u>	<u>N = 1.6</u>
Cx = 1560 m/s	T = 400	T = 700
Cx = 1550 m/s	T = 480	T = 850
$\Delta Cx = 10 \text{ m/s}$	$\Delta T = 80\mu$	$\Delta T = 150\mu$

Thus variation in thickness is more significant when using thin specimens. This is entirely in line with intuition as the variation in thickness will be a greater percentage of the total thickness for a thin specimen.

Skewness of the speed of sound data set distribution, a statistical parameter describing the shape of the distribution, was investigated. The skew values (Table 1) do not appear to have a trend associated with them for either liver or spleen other than that the values are all very close to zero. Thus it would appear that the skew can not be used to discuss the heterogeneity between mouse liver and spleen.

The kurtosis also did not have a definite trend but the values do not deviate much from those of a normal distribution ($a_4 = 3$). Thus any assumptions regarding normality are valid.

Upon inspection of Table 1 it is noted that C_x varies more within the same specimen than the error analysis indicated. Therefore it was necessary to examine further the heterogeneity of the specimens. A t-test for the difference between two independent means (Bruning and Kintz, 1968) to determine if two interference lines yielded a significantly different value for the speed of sound. As mentioned earlier, three different interference lines (lines 15, 20 and 25) were usually examined, with the distance between each of the interference lines being approximately 400 micrometers in the specimen. The t-test indicated that the lines were significantly different, and thus indicating that the speed of sound of the tissue changed over a distance less than 400 micrometers. Taking this one step farther, the t-test was performed on several adjacent lines between 20 and 25 for one sample of each tissue type. This analysis showed that the sound speed changed gradually over 400 micrometers. Thus the values obtained are not a result of error, but rather the inhomogeneity of the tissue.

In conclusion, the automated technique for determining the speed of sound of a specimen does work - the values found are comparable to those found in the literature. The speed of sound data set is determined using parameters now measured and calculated with the aid, and the speed and accuracy, of the computer. This data set is much larger than could be generated manually, thus enabling one to use quantitative statistical parameters to study the degree of tissue specimen heterogeneity.

APPENDIX

DATA COLLECTING PROGRAM

\$BATCH

```

C *****
C
C THIS PROGRAM CAPTURES THE LINE SPECIFIED, COMPUTES THE
C SPEED OF SOUND THROUGH THE TISSUE FOR N POINTS, THE STANDARD
C DEVIATION OF THE SPEED, ARRANGES THE SPEEDS IN SEQUENTIAL
C ORDER FOR THE COMPUTATION OF THE MEDIAN WHICH ULTIMATELY IS
C USED TO COMPUTE THE SKEWNESS OF THE DISTRIBUTION OF SPEEDS,
C AND THE MOMENTS AROUND THE MEAN IS COMPUTED TO DETERMINE THE
C TYPE OF DISTRIBUTION PRESENT.
C
C *****
C INTEGER*4 PBLK(5), LINE(33), CHAR(20)
C INTEGER*2 TIM(482), ARRAY(48), TIMP(482)
C DIMENSION YP(482), DF(482), FN(482), CX(482), AHOLD(482), ICX(482),
C CFREQ(2200)
C WRITE(1,1)
1  FORMAT(' ENTER NUMBER OF POINTS OVER (I2 FORMAT)')
C READ(1,2) I1
2  FORMAT(I2)
C CALL SYSIO(PBLK, Y'58', 4, ARRAY, 96, 0)
C TIM(1)=ARRAY(I1)
C DO 3 J=2,482
C CALL SYSIO(PBLK, Y'58', 4, ARRAY, 96, 0)
C K=1
7  IF(IABS2(TIM(J-1)-ARRAY(K)).LT.8) GOTO 4
C IF(ARRAY(K).NE.0) GOTO 5
C WRITE(1,6)
6  FORMAT('ERROR - THE INITIAL LINE IS NOT CONTINUOUS')
C WRITE(6,6)
C STOP
5  K=K+1
C GOTO 7
4  TIM(J)=ARRAY(K)
3  CONTINUE
C REWIND 4
C CALL SYSIO(PBLK, Y'58', 4, ARRAY, 96, 0)
C IQ=I1+1
C TIMP(1)=ARRAY(IQ)
C DO 8 J=2,482
C CALL SYSIO(PBLK, Y'58', 4, ARRAY, 96, 0)
C K=1
12 IF(IABS2(TIMP(J-1)-ARRAY(K)).LT.8) GOTO 9
C IF(ARRAY(K).NE.0) GOTO 11
C WRITE(1,10)
C WRITE(6,10)
10 FORMAT('ERROR - THE SECOND LINE IS NOT CONTINUOUS')
C STOP
11 K=K+1
C GO TO 12
9  TIMP(J)=ARRAY(K)
8  CONTINUE
C REWIND 4
C WRITE(1,15)
15 FORMAT(' ENTER AVERAGE')
C READ(1,16) IAVE

```

```

16  FORMAT(I2)
    WRITE(1,17)
17  FORMAT(' ENTER TYPE OF SPECIMEN(TITLE)')
    READ(1,18)(CHAR(I),I=1,20)
18  FORMAT(20A4)
    WRITE(6,18)(CHAR(I),I=1,20)
    WRITE(6,19)IAVE
19  FORMAT(' NUMBER OF AVERAGES=',I2)
21  A=0.0
    C=0.0
    D=0.0
    Y=0.0
    N=100
    FF=0.0
    G=0.0
    H=0.0
    S=0.0
    DO 23 I=1,50
      A=A+I
      Y=Y+TIM(I)
      C=C+I**2
      D=D+I*TIM(I)
      FF=FF+I
      S=S+TIMP(I)
      G=G+I**2
      H=H+I*TIMP(I)
23  CONTINUE
    DO 24 I=433,482
      A=A+I
      Y=Y+TIM(I)
      C=C+I**2
      D=D+I*TIM(I)
      FF=FF+I
      S=S+TIMP(I)
      G=G+I**2
      H=H+I*TIMP(I)
24  CONTINUE
    A=A/N
    Y=Y/N
    SL=(D-N*A*Y)/(C-N*A*A)
    FF=FF/N
    S=S/N
    SLO=(H-N*FF*S)/(G-N*FF*FF)
    WRITE(1,89)
    WRITE(6,89)
89  FORMAT(' LINE#          SLOPE          YBAR          XBAR')
    WRITE(6,25)I1,SL,Y,A
    WRITE(1,25)I1,SL,Y,A
25  FORMAT(' ',I3,5X,3(F7.2,4X))
    WRITE(1,89)
    WRITE(6,89)
    WRITE(1,25)IQ,SLO,S,FF
    WRITE(6,25)IQ,SLO,S,FF
    DO 26 M=1,482
      YP(M)=SL*(M-A)+Y
      DF(M)=TIM(M)-YP(M)

```

```

26  CONTINUE
    AD=0.0
    DO 27 M=1,50
      AD=AD+TIMP(M)-TIM(M)
27  CONTINUE
    DO 28 M=433,482
      AD=AD+TIMP(M)-TIM(M)
28  CONTINUE
    AD=AD/N
    DO 29 M=1,482
      FN(M)=DF(M)/AD
29  CONTINUE
    WRITE(1,30)
30  FORMAT(' ', 'ENTER START POINT(I3)')
    READ(1,20)NS
20  FORMAT(I3)
    WRITE(1,31)
31  FORMAT(' ', 'ENTER END POINT(I3)')
    READ(1,20)NE
    QT=NE-NS+1.0
    NQT=QT
    WRITE(6,32)NS,NE,NQT
    WRITE(1,32)NS,NE,NQT
32  FORMAT(' NS=', I3, 2X, 'NE=', I3, 2X, 'N=', I3)
    AVG=0.0
    DO 300 M=NS,NE
      AVG=AVG+FN(M)
300 CONTINUE
    AVG=AVG/QT
    WRITE(1,301)AVG
    WRITE(6,301)AVG
301 FORMAT(' ', 'AVERAGE FN= ', F8.5)
    FNMAX=0.0
    FNMIN=10.0
    DO 302 I=NS,NE
      FNMAX=AMAX1(FNMAX, FN(I))
      FNMIN=AMIN1(FNMIN, FN(I))
302 CONTINUE
    WRITE(1,303)FNMAX, FNMIN
    WRITE(6,303)FNMAX, FNMIN
303 FORMAT(' ', 'FNMAX=', F8.5, 4X, 'FNMIN=', F8.5)
    CT=1507.0
    WRITE(1,33)
33  FORMAT(' ENTER THICKNESS')
    READ(1,34)T
34  FORMAT(F8.5)
    WRITE(6,35)T
35  FORMAT(' THICKNESS(M) =', F8.5)
    THO=0.17837
    H=0.00001507
    TN=SIN(THO)/COS(THO)
    SN=SIN(THO)
    VMAX=0.0
    VMIN=3000.0
    YB=0.0
    SI2=0.0

```

```

AMI4=0.0
DO 36 M=NS,NE
CX(M)=CT*SIN(ATAN(T*SN*TN/(T*SN-FN(M)*H*TN)))/SN
WRITE(1,37)CX(M),T,FN(M)
37 FORMAT(' ',F12.5,1X,F8.5,1X,F8.5)
YB=YB+CX(M)
VMAX=AMAX1(VMAX,CX(M))
VMIN=AMIN1(VMIN,CX(M))
36 CONTINUE
WRITE(1,38)VMIN,VMAX
WRITE(6,38)VMIN,VMAX
38 FORMAT(' VMIN(M/S)=' ,F9.3,3X,'VMAX(M/S)=' ,F9.3)
YB=YB/QT
DO 39 M=NS,NE
SI2=SI2+(CX(M)-YB)**2
AMI4=AMI4+(CX(M)-YB)**4
39 CONTINUE
SI2=SI2/QT
AMI4=AMI4/QT
SI=SQRT(SI2)
WRITE(1,40)YB,SI
WRITE(6,40)YB,SI
40 FORMAT(' AVERAGE SPEED(M/S)=' ,F9.3,3X,'STANDARD DEVIATION(M/S)
C=' ,F9.3)
B2=AMI4/(SI2*SI2)-3.0
IF(B2.LT.0.0) GO TO 43
IF(B2.GT.0.0) GO TO 44
WRITE(1,41)B2
WRITE(6,41)B2
41 FORMAT(' ', 'MESOKURTIC(NORMAL)' ,3X,F6.2)
GO TO 42
43 WRITE(1,100)B2
WRITE(6,100)B2
100 FORMAT(' ', 'PLAYTKURTIC' ,3X,F6.2)
GO TO 42
44 WRITE(1,45)B2
WRITE(6,45)B2
45 FORMAT(' ', 'LEPTOKURTIC' ,3X,F6.2)
42 NEE=NE-1
DO 46 I=NS,NEE
J=I+1
47 IF(CX(I).LE.CX(J))GO TO 48
AHOLD(I)=CX(J)
CX(J)=CX(I)
CX(I)=AHOLD(I)
48 J=J+1
IF(J.LE.NE)GO TO 47
46 CONTINUE
NMED=(NS+NE)/2
AMED=CX(NMED)
WRITE(1,49)AMED
WRITE(6,49)AMED
49 FORMAT(' MEDIAN SPEED(M/S)=' ,F9.3)
TOL=ABS(YB-AMED)
IF(TOL.LT.0.01)GO TO 51
SKEW=3*(YB-AMED)/SI

```

```

IF(SKEW.LT.0.0)GO TO 50
IF(SKEW.EQ.0.0)GO TO 59
WRITE(1,52)SKEW
WRITE(6,52)SKEW
52  FORMAT(' SKEWED RIGHT',F9.3)
GO TO 55
50  WRITE(1,53)SKEW
WRITE(6,53)SKEW
53  FORMAT(' SKEWED LEFT',F9.4)
GO TO 55
51  SKEW=0.0
59  WRITE(1,54)SKEW
WRITE(6,54)SKEW
54  FORMAT(' NORMAL',F9.4)
55  DO 56 I=NS,NE
CX(I)=CX(I)+0.5
ICX(I)=IFIX(CX(I))
56  CONTINUE
IMIN=ICX(NS)
IMAX=ICX(NE)
DO 57 I=NS,NE
J=ICX(I)
FREQ(J)=FREQ(J)+1.0
57  CONTINUE
AMAXX=0.0
DO 58 I=IMIN,IMAX
TRY=FREQ(I)
AMAXX=AMAX1(TRY,AMAXX)
58  CONTINUE
DO 60 I=IMIN,IMAX
IF(AMAXX.NE.FREQ(I))GO TO 60
WRITE(1,61)I,FREQ(I)
WRITE(6,61)I,FREQ(I)
61  FORMAT(' MODE OCCURS AT',I5,'M/S',3X,'VALUE OF',F6.2)
60  CONTINUE
WRITE(6,94)
94  FORMAT(IH0)
DO 63 I=IMIN,IMAX
TRY=FREQ(I)
IF(TRY.NE.0.0)GO TO 64
TRY=1.0
GO TO 65
64  TRY=(TRY/QT)*2000
IF(TRY.LT.1.0) TRY=1.0
65  J=TRY
CALL CLEARL(LINE)
CALL OUTLIN(LINE)
DO 66 K=1,J
66  CALL SETDOT(LINE,K)
63  CALL OUTLIN(LINE)
DO 67 I=1,482
CALL CLEARL(LINE)
IDOT=400+IFIX(64.0*FN(I))
CALL SETDOT(LINE,IDOT)
IF(I.EQ.NS .OR. I.EQ.NE) GOTO 71
GOTO 69

```



```
71  CONTINUE
    DO 68 J=400,600
    CALL SETDOT(LINE,J)
68  CONTINUE
69  CONTINUE
    CALL OUTLIN(LINE)
67  CONTINUE
    WRITE(6,70)
70  FORMAT(1H1)
    STOP
    END
    SUBROUTINE PLTDOT(LINE,IDOT)
    INTEGER LINE(33)
    ENTRY CLEARL
    DO 5 I=1,33
5   LINE(I)=Y'40404040'
    RETURN
    ENTRY SETDOT
    IWD=IDOT/24+1
    IBIT=MOD(IDOT,24)
    IF(IBIT.NE.0) GOTO 6
    IBIT=26
    IWD=IWD-1
    GOTO 8
6   IMOD=MOD(IBIT,6)
    IBYTEE=IBIT/6
    IF(IMOD.EQ.0) IBYTEE=IBYTEE-1
    IBIT=8*IBYTEE+2+MOD(6-IMOD,6)
8   CALL BSET(LINE(IWD),IBIT)
    RETURN
    ENTRY OUTLIN
    IX05=Y'05000000'
    WRITE(6,100) (LINE(J),J=1,32),IX05
100 FORMAT(32A4,A2)
    RETURN
    END
$BEND
```

REFERENCES

- Bruning, James L. and B. L. Kintz (1968). Computational Handbook of Statistics. Scott, Foresman and Company, Glenview, IL, pp. 9-12.
- Foster, S. (1981). An Image Digitizing System of A Scanning Laser Acoustic Microscope. M.S. Thesis, University of Illinois at Urbana-Champaign.
- Frizzell, L. A. and J. D. Gindorf (1981). Measurement of Ultrasonic Velocity in Several Biological Tissues. *Ultrasound in Medicine and Biology*, 7, 385-387.
- Goss, S. A. and W. D. O'Brien, Jr. (1979). Direct Ultrasonic Velocity Measurements of Mammalian Collagen Threads. *J. Acoust. Soc. Am.* 65, 507-511.
- Hoel, P. (1971). Introduction to Mathematical Statistics. John Wiley and Sons, Inc., New York, pp. 170-174.
- Kessler, L. W. and D. E. Yuhas (1979). Acoustic Microscopy 1979, Proceedings of the IEEE, 67, 526-536.
- Mravca. A. (1981). Semi-Automated Techniques to Measure Ultrasonic Propagation Properties Using A Scanning Laser Acoustic Microscope, M.S. Thesis, University of Illinois at Urbana-Champaign.
- O'Brien, W. D., Jr., J. Olerud, K. K. Shung, and J. M. Reid (1981). Quantitative Acoustical Assessment of Wound Maturation with Acoustic Microscopy. *J. Acoust. Soc. Am.* 69, 575-579.
- Spiegel, Murray R. (1961). Schaum's Outline of Theory and Problems of Statistics. McGraw-Hill Book Company, New York.

Teyler, Timothy J. (1980). The Brain Slice Preparation:
Hippocampus. Brain Research Bulletin, 5, 392-403.